JOURNAL OF MATERIALS SCIENCE 24 (1989) 1801–1808

Application of the Weibull statistics to the characterization of metallic glass ribbons

M. CALVO*
Equipe Matériaux Microstructure, ISMRa – Université (CNRS, UA251), 14032 Caen Cedex, France

Metallic glasses are of commercial interest because of their magnetic and mechanical properties. Apart from their embrittlement under given testing conditions which has not yet been fully understood, the ribbons exhibit some inhomogeneities that lead to high failure probabilities for unnotched specimens. Two main types of quenched-in defects can be observed on the rupture surfaces. They are responsible for the specimens failure. For the first time, Weibull theory is successfully applied to the defects distribution in metallic glasses. Three distinct Weibull families of results are distinguished according to Weibull statistics. Two examples of commercial alloys are presented which show the interest of Weibull plots to control the ribbons quality and to follow the evolution of their properties under different conditions of use.

1. Introduction

Metallic glasses are of commercial interest because of their magnetic and mechanical properties. The main problem for their use is their embrittlement which has not yet been perfectly explained. Mechanical investigations have been performed by several authors [1–4] and have revealed that metallic glasses fracture arises (i) for their as-quenched state most of the time in a ductile mode, and (ii) in a brittle mode after annealing or under given testing conditions. Some scatter observed in the measurements of the stress intensity factor K_c and scanning electron microscope (SEM) investigations have revealed ribbons inhomogeneities due to the quenching conditions. As well as for ceramic materials, the existence of such brittle quenched-in defects increases the ribbons failure probability. Tensile tests on unnotched specimens have indeed resulted in a broad distribution of stress values.

Commercial use of metallic glasses would however necessitate the control of the ribbons quality and a possible prediction of their future mechanical behaviour under given conditions of use. Among the statistical methods currently used to the characterization of materials, Weibull statistics has been applied successfully to study flaws distribution in brittle materials such as ceramics [5–11]. Weibull theory is however based on several assumptions so that care must be taken before applying it to stress values distributions.

It will be shown in this paper that Weibull statistics can be applied satisfactorily to metallic glasses although they are not actually brittle materials and that the observed defects can be classified into different Weibull families as presented by Scott and Gaddipati for other materials [12]. The interest of Weibull plots for the control of the ribbons' quality and for the study of the evolution of their properties with different conditions of use will be shown and discussed for several commercial alloys.

2. Materials and experimental techniques

K_c-measurements have been carried out with notched specimens from several types of alloys which have been kindly provided by Allied Chemicals (New Jersey, USA) and Vacuumschmelze (Hanau, FRG). The results obtained with these commercial ribbons have been discussed in previous papers [3, 4, 13]. The composition for which the measurements were obtained in the broadest range (Allied Chemicals MHF 157) has been chosen. The corresponding ribbons were supposed to be the most inhomogeneous and consequently the most suitable for the application of Weibull statistics to the study of quenched-in defects.

A ribbon has been cut in parts 90 cm long, each part being further divided into six specimens. Because the thickness of the ribbons varied from 47 to 57 μm, the location of each specimen within the ribbon width has been carefully noticed. Each specimen width has also been measured after mechanical polishing to avoid any side microcracks due to cutting conditions.

The test fixtures used were identical to those for K_c measurements [3], except for unnecessary Teflon platelets. The mechanical tests have been carried out on a 1195 Instron testing machine and the fracture surfaces observed with an Hitachi scanning electron microscope.

3. Investigation of the inhomogeneity of metallic glass ribbons

3.1. Quenched-in defects

Metallic glass ribbons fracture in their as-quenched state most of the time in plane stress conditions. These

Present address: Laboratoire de Science et Génie des Matériaux Métalliques (CNRS, UA 159) Ecole des Mines, Parc de Saurupt, 54042 Nancy Cedex, France.

0022–2461/89 $03.00 + .12

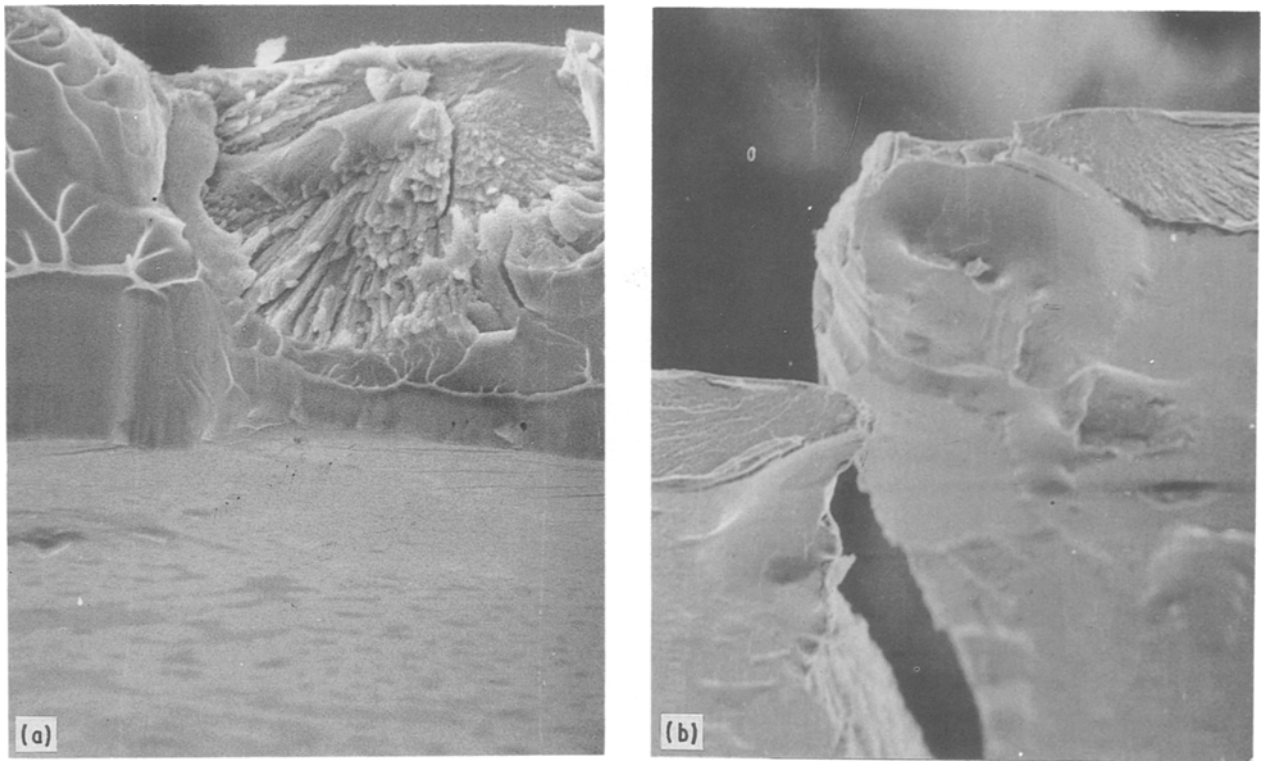

Figure 1 Illustration of the two main defects types observed on rupture surfaces of metallic glass specimens: (a) Type A, (b) Type B.

rupture conditions vary continuously until plane strain conditions when these materials are annealed, even under crystallization, or when they are loaded at very low temperatures or at high strain rates [4, 13, 14]. A dispersion in the toughness values can nevertheless be observed for some types of ribbons and has been linked to the presence of quenched-in defects [4, 15–17]. From the observations of the rupture surfaces of each specimen, notched and unnotched, which had been mechanically tested, two main classes of defects have been distinguished from a shape criterion. They will be called Type A and Type B in the following and are illustrated in Fig. 1.

3.1.1. Type A

The defect shape is clearly defined, with a sharp transition between the defect and the rest of the ribbon which will be called the matrix. X-ray investigations with a Siemens D501 diffractometer and transmission electron microscope observations of such defects have revealed that they form crystallized areas in a still amorphous matrix. These defects are consequently more brittle, in the sense of [13], than the matrix. The surface morphology of these areas confirms this assumption when compared to the ductile (veins pattern) aspect of the matrix.

3.1.2. Type B

The variation between what will be called "the defect centre" and the matrix is smooth and continuous. The sequence of the transition follows the typical morphology evolution observed when the rupture conditions change from brittle to ductile [13]: flat chevrons – rough chevrons – dense veins – less dense veins. Defect of Type B is currently observed near an anomaly of the surface as illustrated in Fig. 1b. Such defects can be due, for example, to a locally reduced rate of the quenching velocity. The observed void can be considered as the trace of an air bubble between the wheel surface and the solidifying ribbon. An insufficient local quenching rate results in a brittle area. When no void can be clearly defined, the orientation of the chevrons pattern indicates a surface defect as the rupture initiation point.

3.2. Analogies with ceramics and brittle composites materials

Defects of Types A and B are currently observed in metallic glass ribbons and SEM observations have revealed that they are most often responsible for the failure of unnotched specimens: they act as brittle areas embedded in a ductile amorphous matrix. The failure analysis has revealed some analogies with ceramics or brittle composites materials:

(1) Metallic glass ribbons which would contain only defects of Type A can be represented as composites: ductile amorphous matrix – brittle areas. Inclusion of defects of Type A into an amorphous matrix fits fairly well with the standard definition of composites materials given by Davis and Bradstreet [18] except of course that the two components, matrix and defects, are not gathered intentionally in order to improve the performance of each component considered separately. This comparison, therefore very attractive, will be used in the following for stress distribution analysis and in another paper [14] for crack propagation interpretation.

(2) The morphology of defects of Type B and the transition from the defect centre to the matrix is reminiscent of fracture mirrors and typical fracture features that can be observed in case of ceramics failure [19].

This comparison and particularly the role of the propagation velocity and strain rate will be used and discussed in another forthcoming paper [14].

Particle distributions, for flaws in ceramics and for one component in composites, are currently characterized by Weibull plots [5–12]. The statistical approach developed by Weibull [20] has been proved to apply perfectly in the case of brittle materials such as ceramics. The results are used to predict the mechanical behaviour and the life time of ceramic materials. Such a rapid characterization applied to the quality control and to the prediction of mechanical behaviour of metallic glass ribbons would be very useful for any commercial production of such materials. Following the two previous analogies, it will be supposed in a first approximation that the existing defects are small enough to consider the toughness as a constant. The rupture stress can be expressed in this case as follows

$$\sigma_r = \frac{K_c}{(\pi a)^{1/2}} \quad (1)$$

where σ_r is the rupture stress, K_c the stress intensity factor already introduced and, a, the crack length.

3.3. Weibull theory

The statistical method commonly used to describe the distribution of fracture stresses in brittle materials is that given by Weibull [20]. His theory is based upon several assumptions:

(1) This first assumption is based on the weakest link of a chain. In Weibull analysis, it is assumed that fracture occurs when the fracture of the weakest link occurs (as opposed to another possible concept implying that fracture of one link causes redistribution of the load among the other links; the fracture then occurs when the overall system cannot resist the redistributed load).

(2) The material is supposed statistically homogeneous at a sufficiently large scale length. The probability to find a critical flaw in a given volume element is the same as for the overall volume.

(3) A stressed solid can fracture, due to any of a series of independent and mutually exclusive mechanisms or causes, each having its own probability of fracture.

From these assumptions, Weibull has considered the failure probability of a volume V of material, in simple tension, under a stress σ, to be given by the following relationship

$$P_f(\sigma) = 1 - \exp\left[-V\left(\frac{\sigma - \sigma_u}{\sigma_0}\right)^m\right] \quad (2)$$

where σ_0 is a scale parameter, m is the Weibull modulus and σ_u is the location parameter i.e. the stress at which there is zero probability of failure. σ_u is often taken equal to zero to obtain reliable safety factors for design [21].

For N identical specimens, the failure probability of the ith one has been set by Weibull to be

$$P_{fi}(\sigma) = \frac{N+1}{N+1-i} \quad (3)$$

or

$$\text{Log Log}\left[\frac{1}{1 - P_{fi}(\sigma)}\right] = \text{Log Log}\left[\frac{N+1}{N+1-i}\right] \quad (4)$$

Equation 3 combined with Equation 2 for $\sigma_u = 0$ results in:

$$\text{Log Log}\left[\frac{N+1}{N+1-i}\right] = m \text{ Log } \sigma_i - m \text{ Log } \sigma_0 + \text{Log } V \quad (5)$$

The parameter m is obtained by plotting the calculated expressions [Log Log $(N + 1/N + 1 - i)$] against the logarithm values of the rupture stress. The N specimens are ordered with increasing stress value so that the Nth specimen corresponds to the highest measured stress value. The slope of the resulting straight line is the Weibull modulus of the distribution.

Several points have however to be verified before assuming that a distribution follows the Weibull statistics and before using the Weibull plots for the material characterization:

(i) there must be a linear relationship between the [Log Log $(N + 1/N + 1 - i)$] and the (Log σ_i) values. The Weibull statistics however, take into account only one type of flaw whereas they can be of several types depending on their composition or their location within the specimen (surface and volume flaws for example). A non-linear distribution can consequently also be due to the simultaneous presence of several types of flaws [10, 12].

(ii) The number of tested specimens must be statistically sufficient to obtain meaningful results by Weibull analysis. The required numbers N corresponding to several m values have been calculated by Jayatilaka and Trustrum [5].

(iii) The volume effect (assumption 2 above) of the Weibull theory must be verified. Let P_f be the failure probability of flaw at a stress σ_1 in volume $V1$ and σ_2 in volume $V2$. Assumption (2) leads to write Equation 5 whatever the flaw i as follows

$$\left(\frac{\sigma_1}{\sigma_2}\right)^m = \frac{V2}{V1} \quad (6)$$

or

$$m \text{ Log } \sigma_1 + \text{Log } V1 = m \text{ Log } \sigma_2 + \text{Log } V2 \quad (7)$$

This equation relates in fact the volume effect.

The plots [Log Log $(N + 1/N + 1 - i)$ against $(m \text{ Log } \sigma_j + \text{Log } V_j)$] must be identical for j equal to 1 and 2. This third check is necessary because the statistical homogeneity of the flaws distribution is not obvious for every material.

4. Results obtained with a Co-based alloy

4.1. Different types of defects

For the application of Weibull statistics to metallic glasses, the most inhomogeneous alloy has been chosen among the ribbons for which K_c-measurements had been previously performed. This alloy was

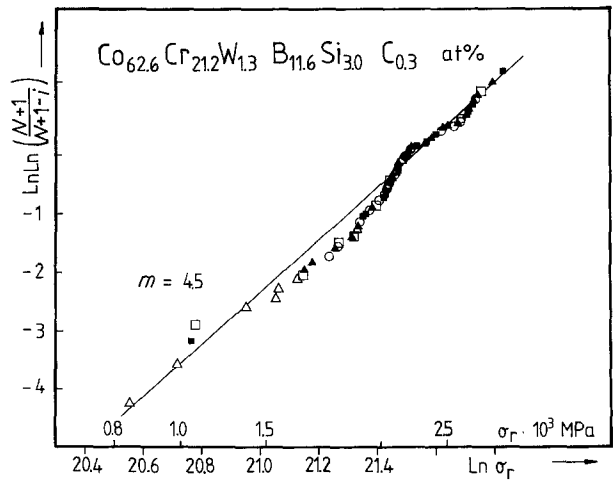

Figure 2 Weibull plot calculated for 71 specimens of a commercial Co-based ribbon. The symbols assigned to each point correspond to the defects that were responsible for the specimens failure: (○) Veins, (■, □) Type A, (▲) Type B-I and (△) Type B-II. $w \simeq 3.7$ to 4.9 mm; $e \simeq 47$ to 57 μm; gauge length = 50 mm.

supposed to contain a lot of quenched-in defects and consequently give rise to a well defined Weibull distribution. Seventy-one specimens have been tested which is a sufficient number for a reliable statistical analysis [5]. The Weibull plot is represented in Fig. 2. The distribution is not linear but the calculated slope of the straight line, that can however be drawn to fit all the data, is 4.5. Such skewed linear distribution recalls the Weibull plots obtained for a combination of a few flaw families, which will be called Weibull families [12].

Careful SEM observations of the specimen rupture surfaces have revealed five types of failure conditions which have been represented with a different symbol in Fig. 2. The defects associated with the failure are of the two types previously presented, Types A and B. These two types have each been divided into two other types corresponding to different surface morphologies. The four resulting defect types are illustrated in Fig. 3. Types B-I and B-II only differ by the size of the surface anomaly at the failure origin. This distinction will be used in the following to classify the specimens according to distinct defect sizes. Types A-I and A-II are similar enough and will not be distinguished in the following. They only differ by the aspect of the brittle area that forms the defect. The specimens for which no brittle areas or defects could be observed on the fracture surfaces have been classified in a 5th type. This 5th type will be called "veins", because the rupture surfaces for these specimens are entirely covered with veins patterns which is the characteristic morphology for metallic glass ductile rupture [3, 22]. The fracture has been in this case most of the time initiated at the specimen sides as was indicated by the presence of numerous shear lines.

These first results require some comments:

(1) The classification in five types of failure conditions goes along with increasing magnitude of the stress values: Type B-I is for example associated with the lowest σ_r values.

(2) Weibull plots calculated for each of the five types separately can however not be perfectly fitted by a straight line.

TABLE I Classification of the different types of defects as a function of the specimen location within the ribbon width

Thickness, e (μm)	Type			
	B-I	B-II	A	Veins
55	4	5	1	2
56	7	1	2	2
57	1	4	7	0
53	1	5	5	1
51	3	2	1	4
47	2	2	0	8

(3) The five different types seem to be distributed in correlation with the specimen location within the ribbon width. Table I summarizes the number of specimens for which the different types of defects have been observed as a function of sample thickness, e, ordered from left to right side of the initial ribbon (top to bottom of Table I). The defects types are ordered with increasing magnitude of stress values (left to right side of Table I).

For the thinner specimens, $e = 47$ and 51 μm, the main type is veins. Good quenching conditions have probably been favoured by the weaker thickness. The middle specimens, $e = 57$ and 53 μm, mainly contain Types A and B-II. Large defects such as Type B-I seem to appear preferentially in thicker side parts of the ribbon, $e = 55$ and 56 μm, where the formation of air bubbles between the wheel and the substrate has been probably more likely to occur.

(4) For a given type, no influence of the specimen location within the ribbon width is however noticeable on the stress distribution. Fig. 4 represents the Weibull plot calculated with all the specimens for which defects of Type B have been observed. The symbols are associated to the average thickness of the corresponding ribbon part where the specimen has been cut. No influence of the specimen location can be noticed.

From the skewed distribution of Fig. 2 it can be supposed that the specimens could be divided into several Weibull families for which the associated Weibull plot would be linear. Comment (1) reveals that this classification, if it is possible, should follow the order of stress values. Comments (2) and (4) show however that these Weibull families are different from the defects types into which the specimens have until now been classified. The morphological criterion alone is consequently not satisfying.

4.2. Volume effect and possible errors

In order to verify the validity of assumption (2) in Weibull theory, a set of 34 specimens similar to the 71 previous ones has been prepared. They have however been tested with a gauge length of 30 cm instead of 50 cm. The Weibull plot calculated for the 34 specimens could be fitted with a straight line with same slope 4.5, but shift towards higher stresses. The common m value has been used to calculate the two plots [Log Log $(N + 1/N + 1 - i)$ against (Log V + m Log σ_r)] for the two sets of specimens. The results are represented in Fig. 5. The two plots are identical

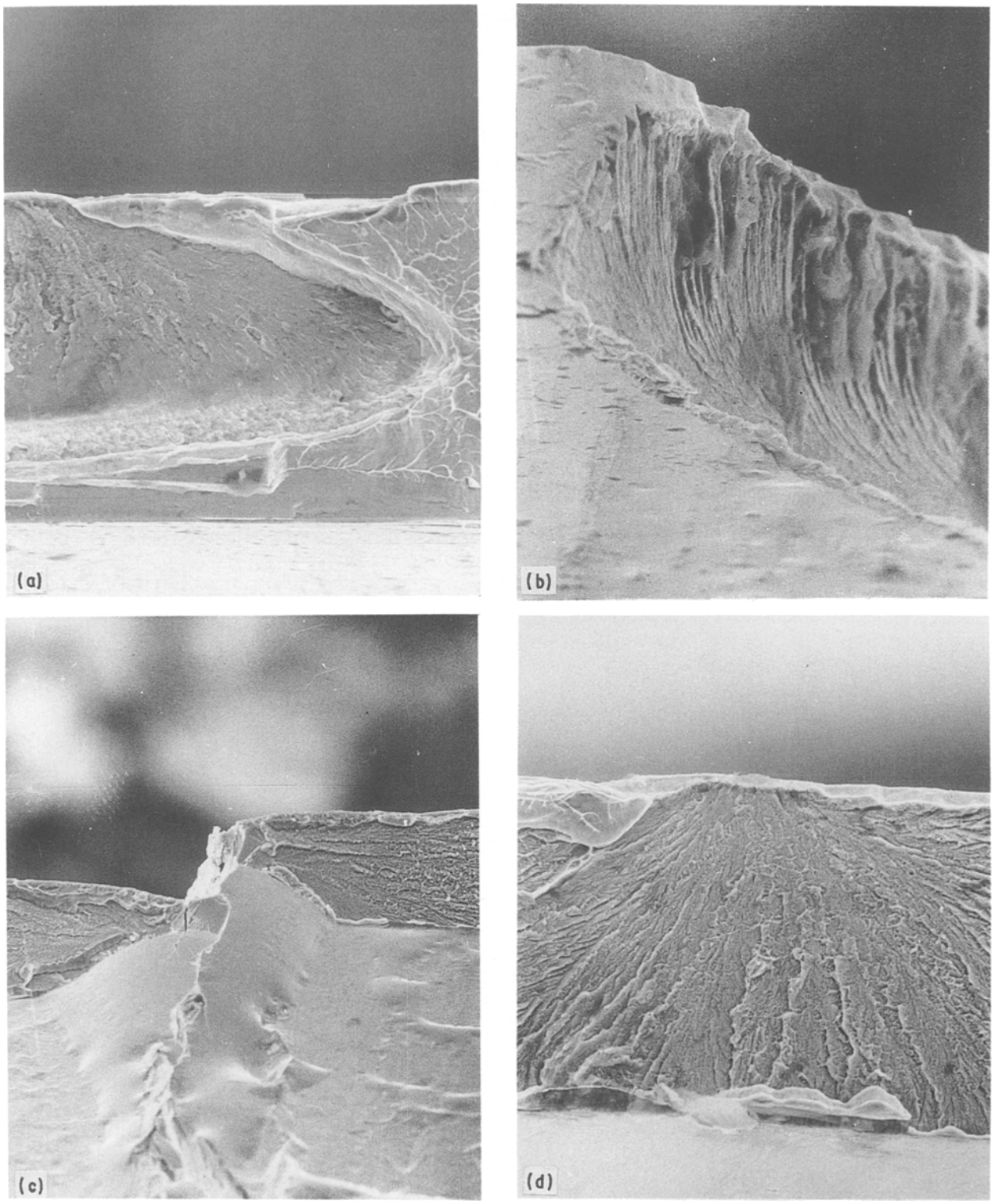

Figure 3 Illustration of the four defects types which have been observed for the Co-based alloy. (a) and (b) are of Type A and (c) and (d) are of Type B. (a): A-I, (b): A-II, (c): B-I, (d): B-II.

and the slope of the resulting straight line is about 1.0 as should be expected by Equation 6.

Although the assumption about the volume effect appears to be verified by the results in Fig. 5, possible errors due to size differences between specimens have been analyzed:

(1) Even in quite good quenching conditions, metallic glass ribbons are not perfectly homogeneous in thickness, particularly within the ribbon width. Fig. 6 reports several series of thickness measurements which have been carried out on the ribbon with a comparator of 0.5 micrometer precision. Each point represents the average value of ten measurements performed in a 1 cm long ribbon part but for the same location within the width. The measurements along the width are distant from about 1 mm. The different symbols in the figure correspond to the different 1 cm long parts randomly located along the ribbon length. From these results an average thickness value has been assigned to each specimen in relation with the ribbon part where it has been cut out. The two extreme values, 47 and 57 μm, correspond to a volume ratio $V1/V2 = 1.213$. The resulting relative difference in

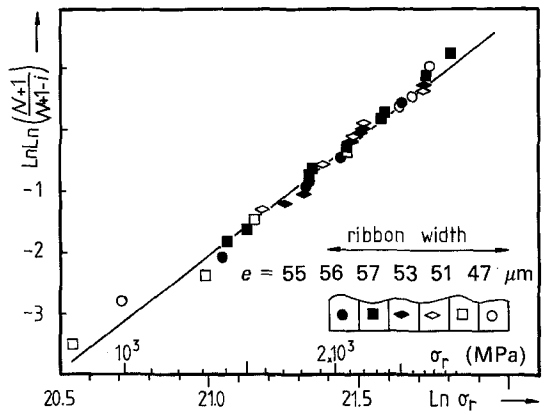

Figure 4 Weibull plot calculated for the specimens for which defects of Type B have been observed. The symbols assigned to each point correspond to the thickness of the ribbon part where the specimen has been cut out. w = 3.7 to 4.9 mm; gauge length 50 mm.

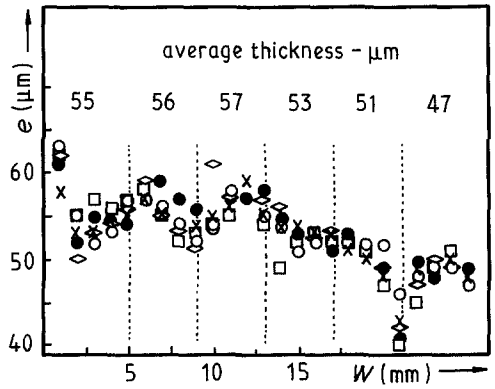

Figure 6 Thickness measurements performed along the ribbon width for several 1 cm long parts randomly located in the ribbon length. The symbols assigned to each point correspond to a different 1 cm long ribbon part.

stress values, calculated with Equation 6, would be 4.4% which is far less than the observed scatter of the Weibull distribution.

(2) Differences in width between specimens have also been observed. It was indeed difficult to prepare specimens with exactly the same geometry. The two extreme reported values, 3700 and 4900 μm, correspond to a volume ratio $V1/V2 = 1.32$ which would result in a stress difference of 6.4%, also smaller than the distribution scatter.

(3) The combined differences in thickness and width have resulted in calculated specimen volumes ranging between 9.5×10^{10} and 1.30×10^{11} μm^3. These two extreme values correspond to a volume ratio $V1/V2 = 1.37$ and a stress difference of 7.2% which is also less than the scatter observed in the specimen stress values.

(4) These calculated specimen volumes are however randomly distributed through the Weibull plot in Fig. 2.

(5) The observed shift in stress values when the gauge length is changed from 50 to 30 cm is about twice the maximum scatter which could be attributed to size differences between the specimens.

From these five results, it may be concluded that the scatter observed in stress values is to be attributed to a Weibull distribution of flaws and not to measurement errors or size differences between specimens.

4.3. Three Weibull families

At this stage, it is obvious that there is not straightforward correspondence between the Weibull families into which the specimens could be classified and the defects types. In a first approximation, K_c has been considered as a constant in Equation 1 because the defects have been supposed to lead to small cracks. To verify if this hypothesis was correct, each defect length has been measured. In the case of Type B defects, the defect area has been considered to be the total area covered with chevrons patterns. In the case of Type A, the defects size is clearly defined. The defect length measured with such a criterion is however overestimated and would better correspond to the crack propagation before catastrophic rupture has occurred [3, 15].

First of all, these defect lengths have been used as crack lengths to estimate the specimens K_c values. The results are represented in Fig. 7 against the defects length.

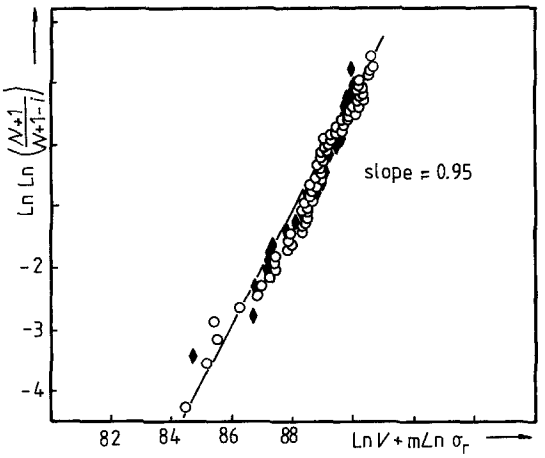

Figure 5 Verification of the volume effect. Two gauge lengths have been used which correspond to two specimens volumes. (○) 50 mm; (◆) 30 mm. The common straight line with a slope of about 1.0 is in agreement with Equation 6. e = 47 to 57 μm, w = 3.7 to 4.9 mm.

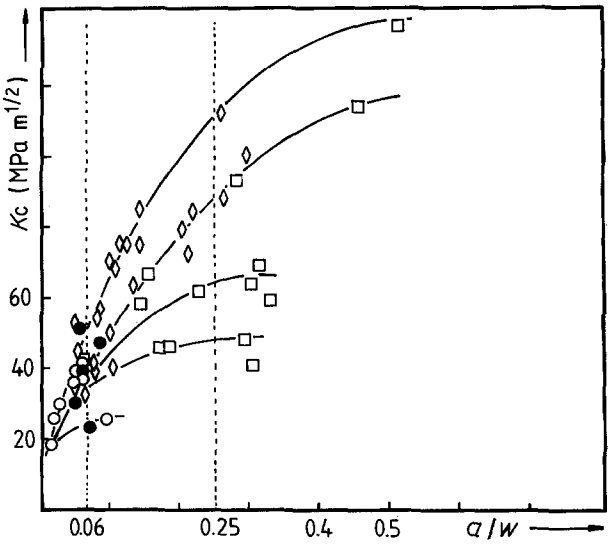

Figure 7 Stress intensity factors calculated for each tested specimen. The symbols assigned to each point correspond to the defects types that has been observed: (●, ○) Type A, (□) Type B-I and (◇) Type B-II. e = 47 to 57 μm; w = 3.7 to 4.9 mm.

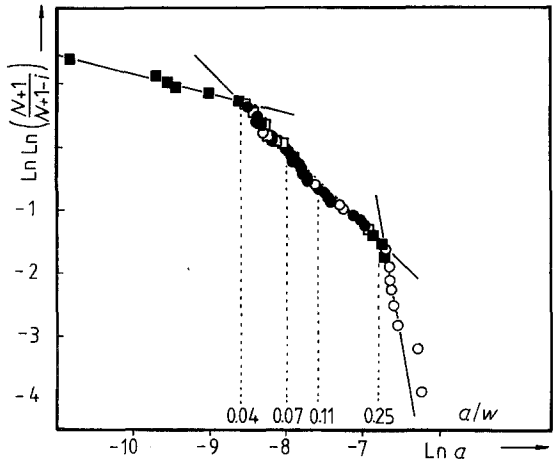

Figure 8 Weibull plots calculated for the defects lengths which have been measured on the specimens rupture surfaces. The symbols correspond to the defects types. (□, ■) Type A, (●) Type B-II, (○) Type B-I. e = 47 to 57 μm; w = 3.7 to 4.9 mm.

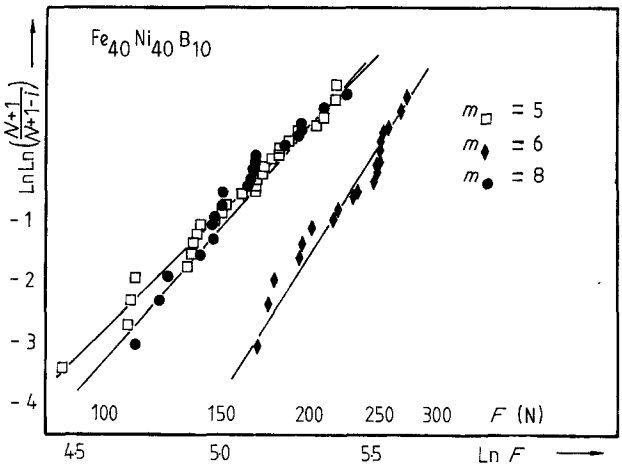

Figure 10 Weibull plots obtained for an Fe-based alloy of commercial origin. The symbols assigned to each point correspond to the different testing conditions. (◆) as-quenched, 77 K (●) as-quenched, RT (□) annealed, 500 K, 3 h, RT. w = 2.9 mm; e = 40 μm; gauge length = 10 mm.

Further on, the defect lengths have been classified in increasing order to calculate the Weibull plot which is represented in Fig. 8. Equation 1 can indeed be written as: Log a = 2 Log K_c − 2 Log σ_r. The plot of [Log Log $(N + 1/N + 1 - i)$] against (Log a) instead of (Log σ_r) has allowed to clearly define three types of failure conditions, which this time correspond to different crack propagation before rupture. The Weibull plots calculated for each of these families separately are represented in Fig. 9. The distributions are now linear with respective slopes of 3, 4 and 6.

These results allow several comments:

(1) The Weibull families defined in Figs 8 and 9 partly correspond to three types of defects: Type A, Type B-I and Type B-II.

(2) As it would have been expected, the longest defects are of Type B-I and their Weibull plot exhibits the minimum slope in Fig. 9 which indicates that the presence of such defects will lead to high failure probability for the specimens. The smallest defects are mainly of Type A and correspond to the maximum slope. The interpretation of crack propagation from these defects needs further developments and will be discussed in another paper in correlation with the overall embrittlement of metallic glasses.

(3) For the middle family ($0.06 < a/w < 0.25$), two curves (K_c against a/w) can be drawn corresponding to the two defects types that can be observed, B-I and B-II. These two toughness levels indicate two ways for crack propagation. Defects of Type B-I lead to lower resistance to crack propagation for the specimens and consequently to higher failure probability.

(4) Within one of these three families, Weibull statistics can be correctly used to characterize the flaws distribution.

5. Discussion and conclusion

From the results presented in this paper, several conclusions can be made:

(1) Weibull statistics applies satisfactorily to the rupture of metallic glass ribbons although they are not actually brittle materials. Care must however be taken to establish the Weibull plots: the number of tested specimens must be sufficiently large for a meaningful statistical analysis and size differences between specimens must be as reduced as possible.

(2) The degree of linearity of the Weibull plots is a good indication of the homogeneity in quenching conditions all over the ribbon. SEM observations of

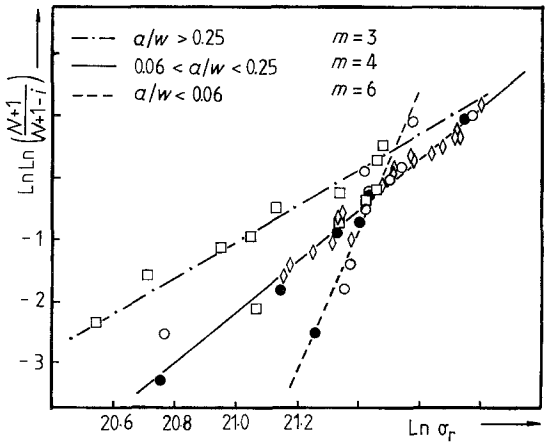

Figure 9 Weibull plots calculated for each range of defects length separately. The three linear distributions correspond to three Weibull families. (●, ○) Type A, (◇) Type B-II, (□) Type B-I. e = 47 to 57 μm; w = 3.7 to 4.9 mm.

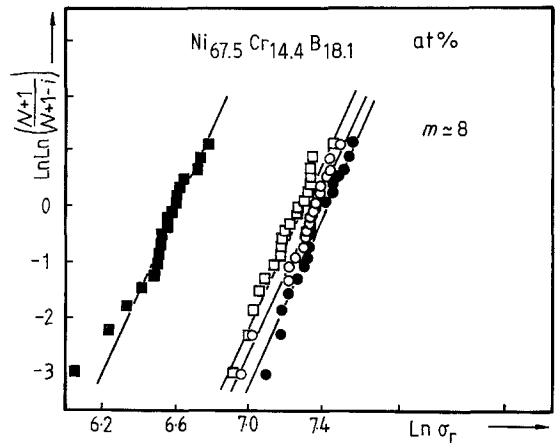

Figure 11 Weibull plots obtained for a Ni-based alloy of commercial origin. The symbols correspond to different testing conditions. As-quenched (○) RT and (●) 77 K. Annealed 573 K 3 h (□) RT and (■) 77 K. e = 32 μm; $w \simeq$ 5 mm; gauge length = 60 mm.

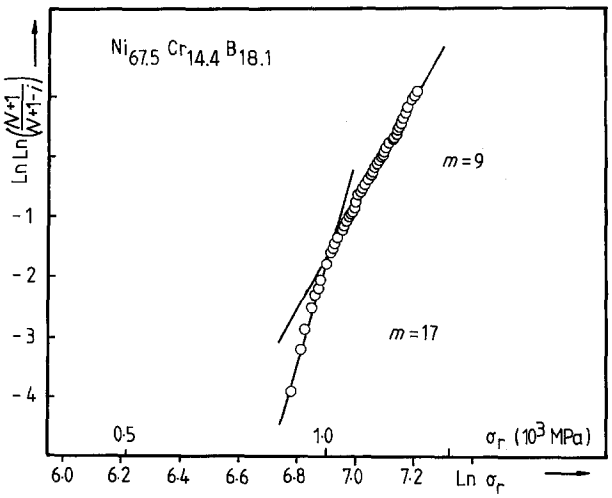

Figure 12 Weibull plot obtained for another ribbon from the same Ni-based alloy as Fig. 11. $w \simeq 8.5$ mm; $e = 32\,\mu$m; gauge length = 50 mm. As-quenched, RT.

several specimens can confirm the presence of quenched-in defects and explain their nature and origins. Weibull plots can consequently be used to control the ribbons quality and its improvement with better quenching conditions. The produced ribbons must be free from large defects of Type B-I which would lead to high failure probability of the specimens.

(3) In the case of ribbons with mainly one Type of defects and corresponding to one Weibull family, Weibull plots can be used to follow the evolution of the ribbons properties under different conditions of use. As an example, Fig. 10 represents Weibull plots obtained for Fe-based specimens of identical geometry but tested under different conditions at room temperature (as-quenched and as-annealed) and at liquid nitrogen temperature (as-quenched). The scatter in K_c values was very small for this alloy which had been considered as quite homogeneous [3]. The quenched-in defects which have however been observed on the rupture surfaces of the unnotched specimens were of Type B-I and B-II. The ribbons were 2.9 mm broad and homogeneous in thickness. Consequently the specimen width was the same as the ribbon width and only the logarithm of the force values have been calculated instead of the stress values. The skewed distribution could be explained by the presence of large defects of Type B-I. The ribbon quality could however not be improved because of its commercial origin. The interpretation of the observed evolution in the defects distribution has been discussed elsewhere [15–17].

(4) Fig. 11 presents another example of the use of Weibull plots to study the evolution of metallic glasses properties. The ribbon used, a Ni-based alloy of commercial origin, contained principally defects of Type A. The distributions are quite linear with a higher slope, except for the shift plot in black squares corresponding to large defects of Type B-I. Their existence has been discussed in another paper in relation to the overall embrittlement of the ribbon at 77 K [17].

Another ribbon of the same alloy and same commercial origin has also been studied. The Weibull plot is represented in Fig. 12. The distribution is skewed and the slope of its upper part is about 8.9. The defects which could be observed on the rupture surfaces were this time of both Types A and B-I. The comparison of Figs 11 and 12, for the same alloy but two different ribbons, show the interest of Weibull plots to control metallic glass ribbons quality.

In summary, it must thus be concluded that the Weibull plots can be successfully applied to commercial metallic glasses to control the ribbons quality, if care is taken for specimens preparation and size measurements.

Acknowledgements

It is my great pleasure to gratefully thank Dr J. L. Chermant, director of the LERMAT in ISMRa – University of Caen, for his interest and encouragements. Thanks are due also to DAAD and DFJW for supporting financially my stays at the Institut für Werkstoffkunde und Werkstofftechnik in Clausthal-Zellerfeld (FRG) where part of the mechanical investigations and SEM observations were performed. I am grateful to Dr F. Osterstock from LERMAT and to Professor Dr R. Pabst, who was at Max Planck Institut in Stuttgart (FRG), for sharing their experience in the application of Weibull statistics to brittle materials.

References

1. H. KIMURA and T. MASUMOTO, in "Amorphous Metallic Alloys", edited by F. E. Luborsky (Butterworths, USA, 1983) p. 187.
2. F. SPAEPEN and A. I. TAUB, in "Amorphous Metallic Alloys", edited by F. E. Luborsky (Butterworths, USA, 1983) p. 231.
3. W. HENNING, M. CALVO and F. OSTERSTOCK, *J. Mater. Sci.* **20** (1985) 1889.
4. M. CALVO, Thèse, University of Caen, France (1986).
5. A. De S. JAYATILAKA and K. TRUSTRUM, *J. Mater. Sci.* **12** (1977) 1426.
6. T. T. SHIH, *Eng. Fract. Mech.* **13** (1980) 257.
7. A. De S. JAYATILAKA, "Brittle Materials" (Applied Science Publishers, London, 1979).
8. S. B. BATDORF, *Nucl. Eng. Design.* **47** (1978) 267.
9. R. E. MEDRANO and P. P. GILLIS, *J. Amer. Ceram. Soc.* **70** (1987) C230.
10. F. OSTERSTOCK, G. VADAM and J. L. CHERMANT, *Mém. Scient. Rev. Met.* **77** (1980) 7.
11. J. J. PETROVIC, *Met. Trans.* **18A** (1987) 1829.
12. W. D. SCOTT and A. GADDIPATI, in "Fracture Mechanics of Ceramics", edited by R. C. Bradt, D. P. H. Hasselman and F. F. Lange, (Plenum, New York, 1978) p. 125.
13. M. CALVO and F. OSTERSTOCK, *Czechos. J. Phys.* **B35** (1985) 337.
14. M. CALVO, to be published.
15. M. CALVO, W. HENNING and F. OSTERSTOCK, in Proceedings of the 5th International Conference on Rapidly Quenched Metals, August, 1984, edited by S. Steeb and H. Warlimont (Elsevier Science, 1985) p. 1385.
16. M. CALVO and F. OSTERSTOCK, *Mém. Et. Scient. Rev. Met.* **82** (1985) 483.
17. F. OSTERSTOCK, M. CALVO, W. HENNING and C. STUTZ, *Int. J. Rapid. Solid.* **3, 4** (1988) 295.
18. L. W. DAVIS and S. W. BRADSTREET, in "Metal and Ceramic Matrix Composites" (Cahners, USA, 1970) p. 1.
19. D. W. RICHERSON, in "Failure Analysis and Prevention" *Am. Soc. Metals, USA*, **11** (1986) p. 744.
20. W. WEIBULL, *Appl. Mech. Rev.* **5** (1952) 449.
21. J. D. SULLIVAN and P. H. LAUZON, *J. Mater. Sci.* **5** (1985) 1245.
22. F. SPAEPEN, *Acta Met.* **23** (1975) 615.

Received 13 May
and accepted 13 September 1988